

Cation dynamics and relaxation in nanoscale polymer electrolytes: A ^7Li NMR study

Piercarlo Mustarelli,* Claudio Capiglia, Eliana Quartarone, Corrado Tomasi, and P. Ferloni
Department of Physical Chemistry, University of Pavia and CSTE-CNR, Via Taramelli 16, 27100 Pavia, Italy

Laura Linati

Centro Grandi Strumenti, University of Pavia, Via Bassi 21, 27100 Pavia, Italy

(Received 16 November 1998; revised manuscript received 17 May 1999)

Composite polymer electrolytes are of interest for solid-state electrochemical devices. In this paper we use ^7Li solid-state NMR to investigate the cation dynamics of poly(ethylene oxide)- (PEO-) based electrolytes, to which nanoscale ceramics has been added. The fillers give origin to nanocomposites. The NMR linewidth is dominated by Li-H magnetic dipolar interaction. The spin-lattice relaxation is chiefly controlled by electric quadrupolar interaction. The spin dynamics is sensibly influenced by the filler nanoparticles, which act as homogenizing agents for the polymer. [S0163-1829(99)05333-3]

I. INTRODUCTION

Poly(ethylene oxide)- (PEO-) based composite polymer electrolytes are currently under investigation for applications in secondary lithium batteries operating above room temperature.¹ In particular, researchers' attention has been focusing on solvent-free, nanoscale materials that seem to offer unique characteristics in terms of high conductivity and both mechanical resistance and interfacial stability.² It is well accepted that nanoscale fillers increase the conductivity of about one order of magnitude with respect to the corresponding micrometric powders.³ Recently, we have shown that the use of fumed silica allows a film $\text{PEO}_8\text{-LiN}(\text{CF}_3\text{SO}_2)_2$ to reach $1.4 \times 10^{-4} \Omega^{-1} \text{cm}^{-1}$ at room temperature.⁴

Whereas the macroscopic effects of nanoscale fillers are becoming well known and easily characterized, a satisfying description of the structure-transport correlations at a microscopic level is still lacking. Only recently, in fact, Dai *et al.* investigated by ^7Li NMR at the magic angle spinning (MAS) the effects of nanoscale MgO and Al_2O_3 on PEO/LiI electrolytes at very high salt concentration.^{5,6} They showed that the addition of quantities of filler of the order 10 vol % leads to more disordered materials in which the crystalline phases are suppressed. Nanocomposites of PEO inserted into layered silicates have been investigated by Wong *et al.*⁷

Among the more common spectroscopic techniques, solid-state NMR is a well-suited tool to investigate both polymer structure and ion dynamics of polyether-based electrolytes. Some relevant studies have been carried out that shed light on the cations motion in the different polymer phases,^{8,9} cation and anion dynamics,^{10,11} nonequivalent lithium sites,¹² and the mechanisms controlling the NMR observables.¹³

In this paper we present a ^7Li solid-state NMR study of the effects of different fillers on PEO-based polymer electrolytes. Both nanoscale silica (an insulator) and lithium triborate sol-gel glass (an ionic conductor) are employed as the filler. LiClO_4 and $\text{LiN}(\text{CF}_3\text{SO}_2)_2$ are used as the electrolyte salt. With the help of ancillary thermal techniques, we get valuable information on the role played by the filler in PEO-based, solvent-free polymer electrolytes.

II. EXPERIMENTAL DETAILS

$\text{LiN}(\text{CF}_3\text{SO}_2)_2$ (Fluka) and CH_3OH (<5 ppm H_2O , Aldrich, 99%) were stored in a dry box and used as received. Poly(ethylene oxide) (BDH Ltd., Polyox WSR-301, molecular weight 6×10^5) was dried for 1 day at 55°C in a oven under vacuum (10^{-2} torr). Anhydrous LiClO_4 (Aldrich, 95%) was dried for 3 days at 140°C in a oven under vacuum (10^{-2} torr). Fumed silica was calcined overnight at 900°C in a quartz tube under N_2 flow. All the thermally treated chemicals were stored in the dry box before use. The lithium triborate sol-gel glass was prepared as described elsewhere.¹⁴

All phases of the samples preparation were performed in the dry box. Stoichiometric amounts of PEO and salts were dissolved in absolute methanol in order to obtain a ratio $n = \text{O}(\text{EO})/\text{Li} = 8$. The required amounts of fumed silica were then added to the solution, which was magnetically stirred for several hours. The solvent was then gently evaporated, and the films were dried at 50°C for 2–3 days. The sample filled with lithium triborate was prepared as described in Ref. 15.

The ^7Li solid-state NMR measurements were performed at 9.4 T with an AMX400WB spectrometer (Bruker, Germany) and a wide line probe. The ^7Li Larmor frequency was 155.6 MHz. The spectra were obtained by a single pulse 90° irradiation (pulse length 5.6 μs). Spin-lattice relaxation times T_1 were obtained by a standard inversion-recovery sequence.¹⁶ Spin-spin relaxation times T_2 were obtained by conventional spin-echo experiments.

Modulated differential scanning calorimetry (MDSC) measurements were performed on samples of about 20 mg under N_2 flow, using a MDSC 2910 interfaced to a TA2000 thermal analysis system (TA Instruments, New Castle, DE, U.S.A.). A period of 40 s, a modulation amplitude of 0.5°C , and a heating rate of $5^\circ\text{C}/\text{min}$ were employed.

III. RESULTS

Figure 1 shows the room-temperature ^7Li line shapes (a) of the sample $(\text{PEO})_8\text{-LiClO}_4$ and (b) of the same sample filled with 33 wt % of $\text{Li}_2\text{O-3B}_2\text{O}_3$. Similar NMR lines were

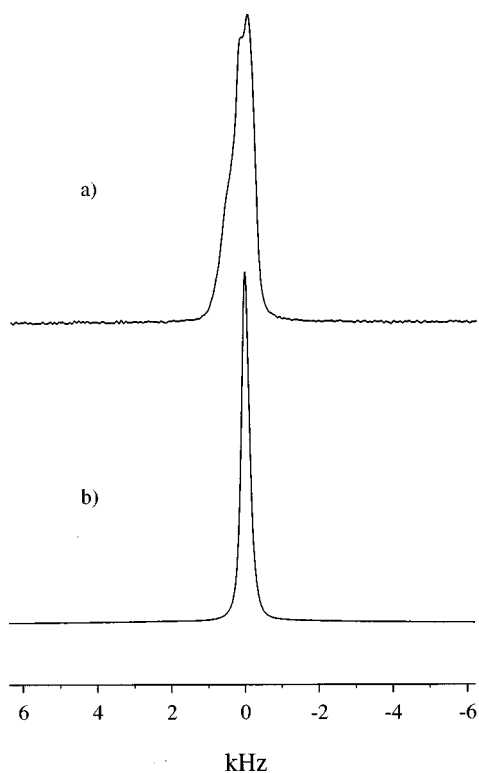


FIG. 1. ${}^7\text{Li}$ NMR line shapes at room temperature (a) of the sample $(\text{PEO})_8\text{-LiClO}_4$ and (b) of the same sample filled with 33 wt % of $3\text{Li}_2\text{O}\cdot 3\text{B}_2\text{O}_3$.

found for all the samples we examined. The spectra chemical shift is ~ 0 ppm. Curve (a) is structured, whereas curve (b) is Lorentzian-Gaussian shaped. The full widths at half height (FWHM) $\Delta\nu$ are 670 Hz for sample (a) and 330 Hz for sample (b), respectively. Since we obtained $T_2 \cong 3.3$ ms for the unfilled electrolyte and $T_2 \cong 2.2$ ms for the filled one, from the relationship $\Delta\nu \cong 1/\pi T_2$ (which holds in the high-temperature region) we can estimate intrinsic linewidths of ~ 100 and ~ 150 Hz, respectively. On the other hand, we estimate the field inhomogeneity of our wide-line probe to be of about 200 Hz, and so we can assign nearly half of the linewidth broadening of curve (a) to the magnetic susceptibility of the sample itself, which is likely related to semimacroscopic inhomogeneities. This contribution to the NMR line seems to be substantially removed by the filler addition (see the following). In principle, the structure of curve (a) could be also explained in terms of a not fully averaged electric quadrupolar interaction. However, the line shape does not change up to 360 K, i.e., well above the relaxation maximum (see Fig. 4) where the correlation time for the cations motion is of the order of 10^{-9} s, which is at least four orders of magnitude shorter than the inverse of the quadrupolar coupling in lithium compounds. Therefore, we can rule out this possibility.

Figure 2 shows the behavior vs temperature of the ${}^7\text{Li}$ NMR linewidth of some selected samples with and without filler. In all cases, the linewidth narrowing is clearly controlled by the polymer glass transition temperature T_g (see Table I), as expected for polyether-based electrolytes where the cations dynamics is strongly coupled with the motions of the chains belonging to the amorphous phases.^{11,13} We note that the room-temperature linewidth of the filled electrolytes

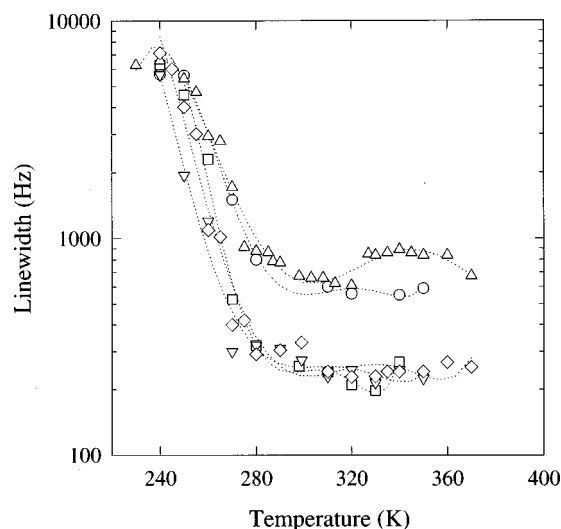


FIG. 2. ${}^7\text{Li}$ NMR linewidth of some selected samples: $(\text{PEO})_8\text{-LiClO}_4$ (up triangles), $(\text{PEO})_8\text{-LiN}(\text{CF}_3\text{SO}_2)_2$ (circles), $(\text{PEO})_8\text{-LiClO}_4$ 10 wt % SiO_2 (down triangles), $(\text{PEO})_8\text{-LiClO}_4$ 33 wt % lithium glass (rhombs), and $(\text{PEO})_8\text{-LiN}(\text{CF}_3\text{SO}_2)_2$ 10 wt % SiO_2 (squares). The lines are only a guide to the eye.

is reduced by a factor of 2–3 with respect to that of the unfilled samples. If we consider the linewidth inhomogeneity of the wide-line probe, we can conclude that line (b) is almost entirely enlarged by residual dipolar coupling and chemical shift.

Figure 3 shows the spin-lattice relaxation rates vs temperature for the samples $(\text{PEO})_8\text{-LiN}(\text{CF}_3\text{SO}_2)_2$ with (squares) and without (circles) 10 wt % of nanoscale SiO_2 . Both curves are peaked at 320 K; the addition of silica determines a $\sim 40\%$ depression of the maximum and an enlargement of the distribution. In addition, it should be noted that the samples, chiefly the unfilled one, exhibit a slope change at near 280 K.

Figure 4 shows the spin-lattice relaxation rates vs tem-

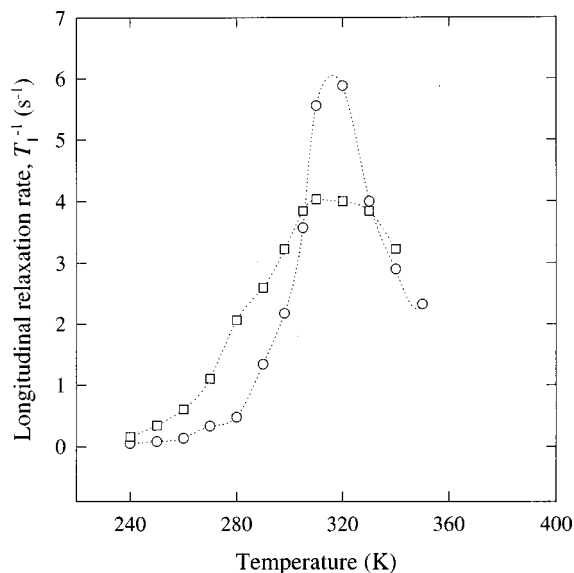


FIG. 3. ${}^7\text{Li}$ spin-lattice relaxation rates vs temperature for $(\text{PEO})_8\text{-LiN}(\text{CF}_3\text{SO}_2)_2$ with (squares) and without (circles) 10 wt % of nanoscale SiO_2 . The lines are only a guide to the eye.

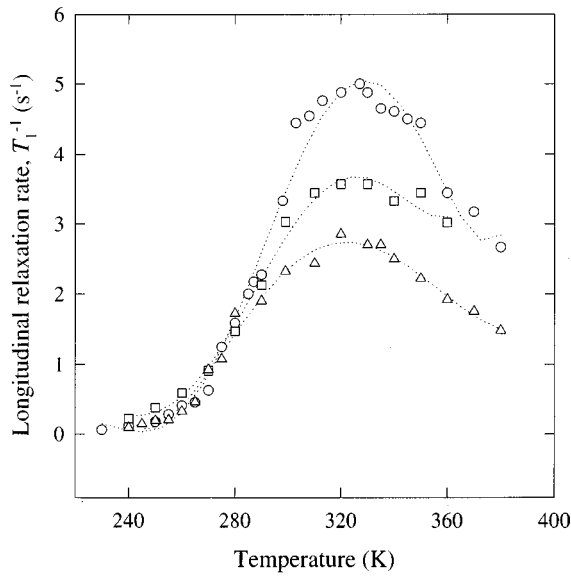


FIG. 4. ${}^7\text{Li}$ spin-lattice relaxation rates vs temperature for $(\text{PEO})_8\text{-LiClO}_4$ without filler (circles), with 10 wt % of nanoscale SiO_2 (squares), and with 33 wt % of triborate glass (triangles). The lines are only a guide to the eye.

perature for the samples $(\text{PEO})_8\text{-LiClO}_4$ without filler (circles), with 10 wt % of nanoscale SiO_2 (squares), and with 33 wt % of triborate glass (triangles). Again, all curves are peaked nearly at the same temperature of 320 K, but the addition of filler causes a relevant dispersion of the relaxation rates above room temperature. In detail, the maxima are depressed by $\sim 30\%$ and $\sim 50\%$ by the addition of silica and glass, respectively. Also, when LiClO_4 is used as the doping salt, a neat slope change appears near 270 K irrespective of filler addition.

Figure 5 shows the MDSC thermograms of some selected samples whose NMR results were presented in the previous figures. The samples do not display melting endotherms be-

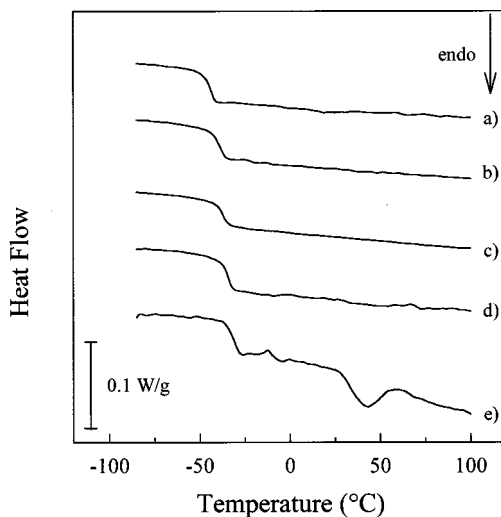


FIG. 5. MDSC thermograms of the same samples reported in Fig. 2. (a) $(\text{PEO})_8\text{-LiN}(\text{CF}_3\text{SO}_2)_2$, (b) $(\text{PEO})_8\text{-LiN}(\text{CF}_3\text{SO}_2)_2$ 10 wt % SiO_2 , (c) $(\text{PEO})_8\text{-LiClO}_4$, (d) $(\text{PEO})_8\text{-LiClO}_4$ 10 wt % SiO_2 , and (e) $(\text{PEO})_8\text{-LiClO}_4$ 33 wt % lithium glass. Just the reversing components are shown.

low 150°C , except for $(\text{PEO})_8\text{-LiClO}_4$ 33 wt % $\text{Li}_2\text{O-3B}_2\text{O}_3$ that shows the melting of a PEO-based crystalline phase (less than 3% of the total, as estimated by the melting enthalpy, $\Delta H_f \cong 6 \text{ J g}^{-1}$). On the other hand, it is well known that $(\text{PEO})_8\text{-LiClO}_4$ is fully amorphous immediately after preparation, while it undergoes partial crystallization in a matter of days.¹⁷ On the basis of these thermal results, the other samples may be considered as fully amorphous, at least at the time when the NMR measurements were carried out.

IV. DISCUSSION

A. NMR linewidth

Figures 1 and 2 show that the addition of fillers plays the main role to homogenize the materials, with no pockets or semimicroscopic fluctuations of the structure, irrespective of the insulating (SiO_2) or conducting (glass) nature of the filler we used. Relevant information on the role played by fillers at the microscopic level may be obtained by investigating the behavior of the ${}^7\text{Li}$ NMR line shape during the transition from the rigid-lattice to the motionally narrowed region.

The NMR motional narrowing takes place when the fluctuations of the local magnetic fields and/or electric field gradients (depending on the nuclear interaction involved) are comparable with the rigid-lattice linewidths. In the case of polyether-based electrolytes, it was shown that the ${}^7\text{Li}$ rigid-lattice linewidth (about 6–7 kHz in PEO-based systems¹⁸) is largely dominated by Li-H magnetic dipolar interaction.¹³ Therefore, the motional narrowing is controlled by the fluctuations of the local magnetic field caused by the Li-H particle-particle correlation function. These fluctuations become relevant at the glass transition due to the setting up of chain-assisted long-range diffusion of the ions. The correlation time of the motional process, τ_c , which at low temperature is of the order of the reciprocal rigid-lattice linewidth Δ_{RL} , is given during the narrowing by the approximate relationship¹⁹

$$\tau_c = \frac{\alpha}{\Delta_{\text{HT}}} \tan \left[\frac{\pi}{2} \left(\frac{\Delta_{\text{HT}}}{\Delta_{\text{RL}}} \right)^2 \right], \quad (1)$$

where Δ_{HT} and Δ_{RL} are the FWHH at a given temperature and in the rigid lattice, respectively, and α is a constant of the order of the unity. If we assume that τ_c is thermally activated,

$$\tau_c = \tau_0 e^{E_{a,n}/kT}, \quad (2)$$

we can obtain the activation energy for the narrowing process, $E_{a,n}$, and the prefactor [or “dwell time” (Ref. 13)] τ_0 , which has the meaning of a reciprocal frequency attempt for cations jumps. The data we obtained by fitting the curves of Fig. 2 are reported in Table I. The addition of the fillers determines the increase of both the characteristic frequency attempt and of the activation energy of the mechanism (the cation motion) that controls the NMR linewidth. We can pictorially say that the filler addition leads to a more disordered and homogeneous material, also in agreement with the results of Dai *et al.*⁶ The apparent paradox of higher conductivity displayed by the samples with higher activation energy^{4,15} simply means that the entropic contribution (related to τ_0) is prevalent on the enthalpic one (related to $E_{a,n}$).

TABLE I. T_g (K): glass transition temperatures detected by MDSC experiments. τ_0 (s): prefactor obtained from Eq. (2). $E_{a,n}$: activation energy for NMR linewidth narrowing, obtained from Eq. (2). $E_{a,r,LT}$: activation energy for spin-lattice relaxation, as obtained from low temperature side of the T_1 curves. $E_{a,r,HT}$: activation energy for spin-lattice relaxation, as obtained from high temperature side of the T_1 curves. $E_{a,\sigma}$: activation energy for conduction, obtained from conductivity measurements.

Sample	T_g (K)	τ_0 (s)	$E_{a,n}$ (eV)	$E_{a,r,LT}$ (eV)	$E_{a,r,HT}$ (eV)	$E_{a,\sigma}$ (eV)
(PEO) ₈ -LiClO ₄	227	3.67×10^{-14}	0.40	0.39	0.12	0.44 ^a
(PEO) ₈ -LiN(CF ₃ SO ₂) ₂	226	3.02×10^{-14}	0.41	0.43	0.20	0.60 ^a
(PEO) ₈ -LiClO ₄ 10 wt % SiO ₂	229	2.06×10^{-17}	0.55	0.28	^b	0.55 ^a
(PEO) ₈ -LiN(CF ₃ SO ₂) ₂ 10 wt % SiO ₂	224	1.11×10^{-17}	0.57	0.36	^b	0.71 ^a
(PEO) ₈ -LiClO ₄ 33 wt % lithium glass	228	1.14×10^{-19}	0.66	0.40	0.13	0.81 ^c

^aData taken from Ref. 4. The conductivity behaviors are Arrhenius like. A 10% error is estimated.

^bFew points for a good fit.

^cValue extracted over the temperature range 300–350 K, where the conductivity can be approximated to be Arrhenius like.

From a microscopic point of view, the prevalence of the entropic term suggests that fillers open up new pathways for the ions to diffuse in the materials or make the existing ones more “efficient.” This can be accomplished by keeping the PEO chains further apart from one another or, also, by forming high-conductivity paths along the dispersoid interface (space charge model²⁰). This point will be further addressed in the next section.

B. Relaxation

It is commonly accepted that spin-lattice relaxation in these polymer electrolytes is dominated,¹³ or at least influenced,¹¹ by the electric quadrupolar interaction between the ⁷Li and the electric field gradient tensor (efg). For a single quadrupolar nucleus of spin I the spin-lattice relaxation rate T_1^{-1} , when the molecular motions can be approximated by a isotropic tumbling with correlation time τ_c , is given by²¹

$$T_1^{-1} = \frac{3\pi^2}{10} \frac{2I+3}{I^2(2I-1)} C_{QQ} \left(1 + \frac{1}{3} \eta^2\right) \tau_c, \quad (3)$$

where C_{QQ} is the quadrupolar coupling constant and η is an asymmetry parameter ranging between 0 and 1. If we take $C_{QQ} \sim 30$ kHz, as suggested by the low-temperature line shapes of our samples, and $\tau_c \cong 10^{-9}$ s, which is reasonable in the extreme narrowing region, we obtain $T_1^{-1} \cong 3.8$ s⁻¹, in agreement with the values of the relaxation maxima displayed in Figs. 3 and 4. Just as a comparison, relaxation rate maxima of 10 s⁻¹ were reported by Gang *et al.* in their study of (PEO)₈-LiClO₄ filled with γ -LiAlO₂.²² Since the magnetic dipolar contributions to the relaxation are generally weaker by at least one order of magnitude in these systems,¹³ our results confirm that quadrupolar interaction dominates the ⁷Li spin-lattice relaxation.

Let us now examine in detail the relaxation behaviors depending on the salt and filler we employed. In all cases, the addition of filler determines a broadening of the relaxation peaks in the high-temperature region, which is associated with an average reduction of the relaxation rates. The broadening induced by the filler is more evident when LiN(CF₃SO₂)₂ is used as the doping salt. For a system of

spin-3/2 interacting nuclei at a temperature T , under a magnetic field $B = \gamma/\omega$, the relaxation rate may be expressed as

$$T_1^{-1}(\omega, T) = AJ(\omega, T) + KC_{QQ}^2 \quad (4)$$

where A measures the dipole-dipole interaction, K is a constant, and $J(\omega, T)$ is a spectral density which depends on the Larmor frequency ω and on the parameters characterizing the motion. While in diluted, weakly interacting systems the spectral density is generally given by the Fourier transform of a single exponential correlation function [the Bloembergen-Purcell-Pound (BPP) model²³], in many complex condensed-matter systems this assumption may be no longer valid because of low-dimensionality effects,²⁴ nonrandom ion motions,²⁵ or even the absence of a characteristic time scale.²⁶ The experimental deviations from the BPP model may be accounted for by introducing distributions of the correlation function (Cole-Cole, Cole-Davidson, and Havriliak-Negami expressions²⁷). Other phenomenological expressions, like the Kohlrausch-William-Watts expression,²⁸ were also employed in data fitting.

The relaxation curves of Figs. 3 and 4 are far from the symmetrical shapes described by the BPP model. On the other hand, a composite polymer electrolyte is a quite complex system, for which the task to associate a physical meaning to the phenomenological expressions^{27,28} is difficult. Therefore, we prefer to simply state that the broadening of the relaxation curves is due to a spread of the distribution of the correlation functions modulating the spin dynamics. From a microscopic point of view, this implies that the fillers add disorder to the polymer structure, which is also in agreement with the increase of the dwell time for the ion hopping obtained by fitting the line-shape narrowing process (see Table I).

Figure 6 shows the room-temperature ⁷Li spin-lattice relaxation rate as a function of the silica content in (PEO)₈-LiClO₄, compared with the behavior of bulk observables, namely, the heat capacity jump at the glass transition, ΔC_p , and the electric conductivity σ . In the limits of the experimental uncertainty, all the reported quantities display a maximum in the range 5–8 wt % of filler content, which means that the filler distribution controls both the thermal and transport properties of these polymer electrolytes. The

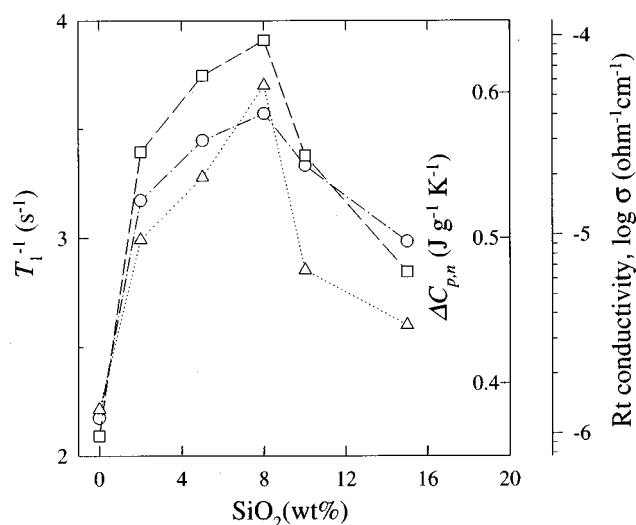


FIG. 6. Behavior vs the silica content of spin-lattice relaxation rate (circles) change of the heat capacity at the glass transition normalized to the actual PEO-salt content, $\Delta C_{p,n}$ (triangles) and conductivity at room temperature (squares). Both the thermal and the conductivity data are taken from Ref. 4. The lines are only a guide to the eye.

maxima of conductivity upon filler addition have been explained²⁹ as the result of two competing effects: (i) the increase of the polymer amorphous phase and (ii) the dilution of the highly conducting amorphous phase with the insulating ceramic material. However, we see from Fig. 5 that our electrolytes are almost completely amorphous, irrespective of the presence of the filler. Therefore, the behavior of ΔC_p must reflect the increase of the degrees of freedom which become motionally active at the glass transition. In other words, the addition of filler makes the polymer more “fragile” in the sense of Angell’s definition,³⁰ which relates the fragility of a glass to its connectivity: the more “connected” the glass is, the less fragile it is. Since the addition of a filler cannot influence the chain length distribution of the polymer, we can conclude that nanoscale silica enters the PEO strands and weakens the glass structure by loosening the coordination bonds Li-O(PEO). Our picture is in agreement with the model proposed by Wiczorek and Siekierski,³¹ who connected the enhancement of conductivity with the existence of a space-charge layer at the polymer-filler interface. This layer is characterized as an amorphous

polymer phase exhibiting a conductivity higher than that of the matrix polymer electrolyte. At silica concentrations higher than 10–15 wt % dilution effects take place that slow down the cations dynamics, as demonstrated by the decrease of T_1^{-1} and σ , and increase the glass strength through more intense Li-O couplings.

From the relaxation curves of Figs. 3 and 4, the activation energies for the low- and high-temperature sides, $E_{a,r,LT}$ and $E_{a,r,HT}$, were extracted. The values are reported in Table I. The values of $E_{a,r,LT}$ for the unfilled samples are in good agreement with those obtained from Eq. (2), which means that the same mechanism (the cation diffusion) is probed by both line-shape narrowing and spin-lattice relaxation. When the filler is added, in contrast, the activation energies from relaxation are left substantially unaffected, while the $E_{a,n}$ ’s increase by roughly 50%. This is further evidence that (i) filler is well distributed in the host polymer and (ii) spin-lattice relaxation is quadrupolarly controlled. In fact, the filler grains are supposed to chiefly influence the magnetic dipolar coupling, which is described by a long-range particle-particle correlation, rather than the quadrupolar one, which is described by a short-range particle-site correlation.

Finally, the activation energies extracted from the high-temperature side of the relaxation curves, $E_{a,r,HT}$, are notably lower than those obtained from conductivity, $E_{n,\sigma}$ (see Table I). This confirms that the spin-lattice relaxation probes the short-range motions rather than long-range diffusion of lithium, and it warns us about a naive use of the data obtained from NMR relaxation.

V. CONCLUSIONS

We used ⁷Li, wide-line solid-state NMR to investigate the cations dynamics in composite polymer electrolytes. The following remarks can be made.

(1) The addition of filler contributes to the homogenization of the electrolyte over a semimacroscopic scale.

(2) The spin dynamics is notably affected by the fillers. The NMR observables, linewidths, and relaxation rates are controlled by magnetic dipolar and electric quadrupolar interactions, respectively.

(3) The activation energies obtained from the relaxation curves in the extreme narrowing region are lower than the corresponding quantities extracted from conductivity data, because the NMR quadrupolar probe is chiefly sensitive to the short-range motions of the cations.

*Author to whom correspondence should be addressed. Electronic address: mustarelli@matsci.unipv.it

¹W. Wiczorek, *Composite Polyether Based Electrolytes* (Oficina Wydawnicza Politechniki Warszawskiej, Warszawa, 1995).

²E. Quartarone, P. Mustarelli, and A. Magistris, *Solid State Ionics* **110**, 1 (1998).

³F. Croce, G. B. Appetecchi, L. Persi, and B. Scrosati, *Nature (London)* **394**, 456 (1998).

⁴C. Capiglia, P. Mustarelli, E. Quartarone, C. Tomasi, and A. Magistris, *Solid State Ionics* **118**, 73 (1999).

⁵Y. Dai, Y. Wang, S. Greenbaum, S. A. Bajue, D. Golodnitsky, G. Ardel, E. Strauss, and E. Peled, *Electrochim. Acta* **43**, 1557 (1998).

⁶Y. Dai, S. Greenbaum, D. Golodnitsky, G. Ardel, E. Strauss, E. Peled, and Yu. Rosenberg, *Solid State Ionics* **106**, 25 (1998).

⁷S. Wong, R. A. Vaia, E. P. Giannelis, and D. B. Zax, *Solid State Ionics* **86-88**, 547 (1996).

⁸D. P. Tunstall, A. S. Tomlin, J. R. MacCallum, and C. A. Vincent, *J. Phys. C* **21**, 1039 (1988).

⁹C. Berthier, W. Gorecki, M. Minier, M. B. Armand, J. M. Chabagno, and P. Rigaud, *Solid State Ionics* **11**, 91 (1983).

¹⁰W. Gorecki, P. Donoso, C. Berthier, M. Mali, J. Roos, D. Brinkmann, and M. B. Armand, *Solid State Ionics* **28-30**, 1018 (1988).

¹¹J. P. Donoso, T. J. Bonagamba, H. C. Panepucci, L. N. Oliveira,

- W. Gorecki, C. Berthier, and M. Armand, *J. Chem. Phys.* **98**, 10026 (1993).
- ¹²J. F. O'Gara, G. Nazri, and M. MacArthur, *Solid State Ionics* **47**, 87 (1991).
- ¹³S. H. Chung, K. R. Jeffrey, and J. R. Stevens, *J. Chem. Phys.* **94**, 1803 (1991).
- ¹⁴P. Mustarelli, E. Quartarone, C. Tomasi, and A. Magistris, *J. Non-Cryst. Solids* **215**, 51 (1997).
- ¹⁵P. Mustarelli, E. Quartarone, C. Tomasi, and A. Magistris, *Solid State Ionics* **86-88**, 347 (1996).
- ¹⁶See, for example, C. A. Fyfe, *Solid State NMR for Chemists* (C.F.C. Press, Guelph, Canada, 1983).
- ¹⁷P. Ferloni, G. Chiodelli, A. Magistris, and M. Sanesi, *Solid State Ionics* **18&19**, 265 (1986).
- ¹⁸See, for example, S. Panero, B. Scrosati, and S. G. Greenbaum, *Electrochim. Acta* **37**, 1533 (1992).
- ¹⁹A. Abragam, *The Principles of Nuclear Magnetism* (Clarendon, Oxford, 1961).
- ²⁰T. Jow and J. B. Wagner, Jr., *J. Electrochem. Soc.* **126**, 163 (1979).
- ²¹R. K. Harris, *NMR and the Periodic Table* (Academic, London, 1978), p. 17.
- ²²W. Gang, J. Roos, D. Brinkmann, F. Capuano, F. Croce, and B. Scrosati, *Solid State Ionics* **53-56**, 1102 (1992).
- ²³N. Bloembergen, E. M. Purcell, and R. V. Pound, *Phys. Rev.* **73**, 679 (1948).
- ²⁴D. Brinkmann, *Magn. Reson. Rev.* **14**, 101 (1989).
- ²⁵K. Funke and I. Riess, *Z. Phys. Chem., Neue Folge* **40**, 217 (1984).
- ²⁶S. Dattagupta, *Relaxation Phenomena in Condensed Matter Physics* (Academic, New York, 1987).
- ²⁷P. A. Beckmann, *Phys. Rep.* **171**, 85 (1988).
- ²⁸G. Williams and D. C. Watts, *Trans. Faraday Soc.* **66**, 80 (1970).
- ²⁹F. Capuano, F. Croce, and B. Scrosati, *J. Electrochem. Soc.* **138**, 1918 (1991).
- ³⁰C. A. Angell, *J. Non-Cryst. Solids* **131-133**, 13 (1991).
- ³¹W. Wiczcerek and M. Siekierski, *J. Appl. Phys.* **76**, 2220 (1994).